

Multilevel Resonant Tunneling through Purely Organic Radical Molecules in a Si-Based Double-Tunnel Junction

Jayanta Bera, Mikhail Kabdulov, Yutaka Wakayama, Thomas Huhn,* and Ryoma Hayakawa*

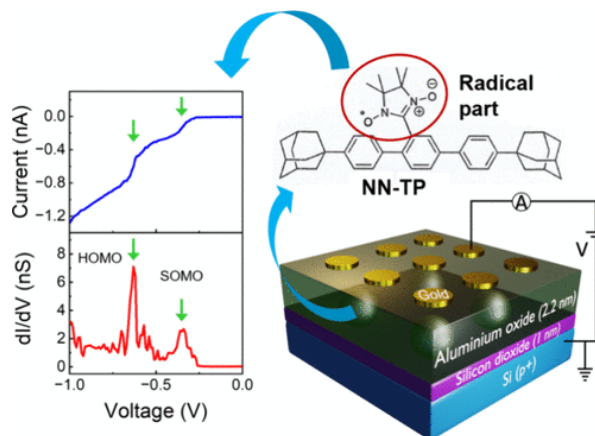
ABSTRACT: The use of purely organic radicals is promising, especially for future applications in molecular spintronics. However, the techniques used to form their molecular junctions, including break-junction and scanning tunneling microscopy techniques, are unsuitable for the integration of molecular devices in a large-scale setting.

In this study, a Si-based double-tunnel junction with purely organic radicals, where adamantyl nitronyl nitroxide p-terphenyl (NN-TP) molecules are embedded as quantum dots in the oxide layer of a metal–oxide–semiconductor (MOS) structure, was demonstrated. Notably, this MOS structure functions as a tunnel junction, which has a high affinity for the current Si technology. In this study, multilevel resonant tunneling through the discrete energy levels of the NN-TP molecules at 7 K was achieved; moreover, the tunneling current was observed at 100K. Furthermore, our device exhibited resonant tunneling through a singly occupied molecular orbital, indicating the survival of an unpaired electron in the radical molecules. Thus, our findings hold promise for incorporating the attractive functions of organic radicals into Si-based solid-state devices, thereby enabling the large-scale integration of molecular devices.

KEYWORDS: organic radicals, resonant tunneling, molecular orbitals, double-tunnel junctions, unpaired electron, quantum transport

1. INTRODUCTION

In recent decades, global digital information has been rapidly growing because of the emergence of the modern big data era and the Internet of Things.^{1,2} However, the use of conventional electronic devices is declining owing to theoretical and physical limits upon downscaling to a few nanometers.^{3,4} As transistors shrink, quantum effects, such as quantum tunneling, quantum interference, and energy-level quantization, become increasingly pronounced.⁵ Therefore, designing nanoscale memory and logic devices based on such quantum effects is becoming increasingly crucial in the construction of energy efficient and



high-speed integrated circuits beyond the ability of the current complementary metal–oxide–semiconductor (CMOS) devices.

Based on this, molecular devices, where in a few molecules are utilized as nanoscale diodes,^{6–8} transistors,^{9–11} resistors,¹² and switches, are promising contenders.^{13,14} Beyond these efforts, the development of molecular-scale spintronic devices has received considerable attention. Purely organic radicals are new building blocks for spintronic applications owing to the following attractive features. First, the molecules comprise light elements and have weak spin–orbit coupling and weak hyperfine interactions. Thus, the spin coherence in organic radicals is preserved for a long time,^{15,16} which is applied to molecular spin–based quantum computing.^{17–19} For example, the molecular spins of TEMPO radical–based self-assembled monolayers (SAMs) were used as quantum bits in a recent study. The spin coherence was preserved at a temperature of up to 60 K.²⁰ Second, the unpaired electrons of organic radicals cause spin-dependent transport of carriers through singly occupied molecular orbitals (SOMOs) or singly unoccupied molecular orbitals (SUMOs), resulting in large magnetoresistance (MR) and the Kondo effect.^{21–24}

Often, quantum transport through a few radical molecules has been evaluated using scanning tunneling microscopy (STM)^{25–30} and break-junction techniques.^{31–38} The unpaired electrons of neutral polychlorotriphenylmethyl radical molecules have been detected concerning Kondo resonance in mechanically controllable break junctions (MCBJs) and electromigration break junctions.^{22,23} Large positive MR has been observed in a single TEMPO–OPE junction formed by the MCBJ technique.²⁴ However, these techniques are unsuitable for large-scale integrated molecular devices owing to their poor compatibility with current CMOS technology and thus are far from use in practical applications.^{39–41}

To overcome the issue aforementioned issue, we have established a unique technique to facilitate quantum transport through a few molecules in a CMOS-compatible device. In our device, the isolated molecules are embedded in the oxide layers of the MOS structure, thus behaving as a double-tunnel junction.⁴² Thus far, single-electron tunneling (SET) or resonant tunneling has been achieved in the samples with C₆₀ or copper phthalocyanine molecules.⁴² Thus far, single-electron tunneling (SET) or resonant tunneling has been achieved in samples with C₆₀ or copper phthalocyanine molecules.⁴² Furthermore, such tunneling current was visible in photoisomerizable diarylethene molecules;⁴³ in particular, the tunneling current was reversely controlled via the photoisomerization reaction of the diarylethene molecules. These investigations were further extended to a vertically formed tunnel transistor, where the MOS

structure with C₆₀ molecules functioned as the transistor channel. The quantum transport that reflected the discrete energy levels of C₆₀ molecules was effectively controlled by the surrounding gate electrode.⁴⁴

In this study, quantum transport through purely organic radicals in a Si-based double-tunnel junction was demonstrated, where adamantyl end-capped *p*-terphenyl nitronyl nitroxide (NN-TP) molecules were used (**Figure 1**). The NN group is known as a stable radical π -conjugated to the host *p*-terphenyl molecules. This feature is expected to induce spin-dependent quantum transport in the associated solid-state device. First, multilevel resonant tunneling through the discrete molecular orbitals (MOs) of the NN-TP molecules at a temperature of 7 K was recognized. Thus, the tunneling current was further maintained at 100 K. Notably, we successfully observed the resonant tunneling via SOMO, which proves the survival of the unpaired electrons of the radical molecules embedded in the device. This could potentially facilitate the integration of unique spintronic functions originating from organic radicals into nanoscale devices for future large-scale applications.

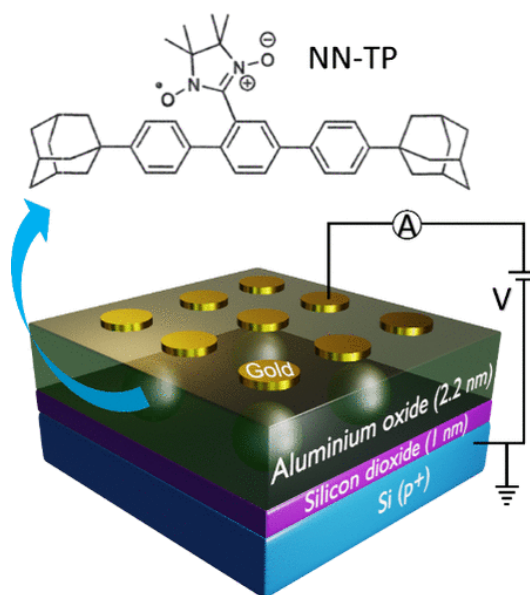


Figure 1. Molecular structure of NN-TP and schematic illustration of the double-tunnel junction based on the Si MOS structure. The isolated molecules were incorporated into the device as quantum dots.

2. RESULTS AND DISCUSSION

2.1. Theoretical Calculation of the MOs of NN-TP. The MOs of the NN-TP molecules were calculated using density functional theory (DFT)⁴⁵ with the BP86 (GGA)⁴⁶ functional and the def2-TZVP basis set in the ORCA package.⁴⁷ Grimme's D3 dispersion

correction using Becke–Johnson damping was considered in the calculations.⁴⁸ Structural geometry was optimized until the energy gradient reached below 10^{-4} Hartree/Bohr; moreover, the change in energy for the SCF iterations was set to 10^{-6} Hartree. Isosurface values were set to 0.02 a.u. for plotting the MOs and 0.003 a.u. for plotting the spin density. **Figure 2a** shows the optimized structure of the NN-TP molecule with the radical part. **Figure 2b** illustrates the calculated MOs with the corresponding energy states for spin up (α) and spin down (β). The energy values of the MOs are presented in **Table S1** in the Supporting Information. The highest occupied molecular orbital (HOMO) and lowest unoccupied molecular orbital (LUMO) are mainly localized on the host benzene rings. Two intermediate orbitals (SOMO and SUMO) are localized on the radical part. This is because of the presence of one unpaired electron in the oxygen atom in the radical part. The energy levels of the SOMO and SUMO are located in the HOMO–LUMO gap. The theoretically estimated HOMO–LUMO gap is 3.25 eV. In contrast, neither a SOMO nor a SUMO exists in the host molecules without the radical part (**Figure S5**). The spin density plot (**Figure 2c**) demonstrates the delocalization of the spin cloud over both oxygen atoms in the radical part, thereby confirming that the SOMO and SUMO originate from the radical part rather than from the host benzene rings. Accordingly, the observation of quantum transport through the SOMO or SUMO energy levels of the NN-TP molecule was the target of this study.

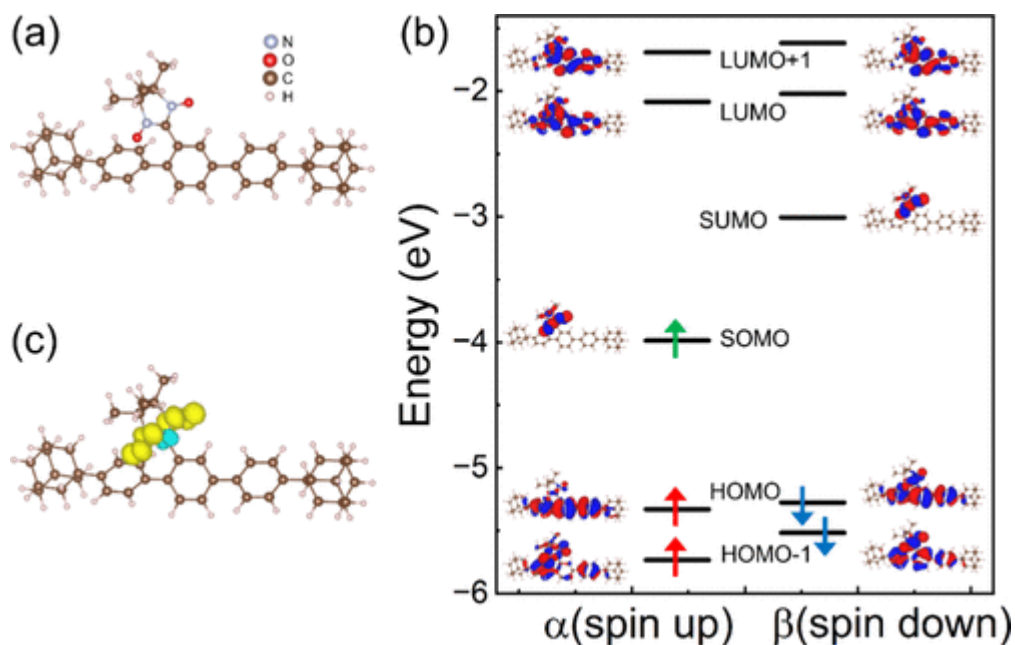


Figure 2. (a) Optimized molecular structure, (b) energy levels of the MOs, and (c) spin density plot of NN-TP obtained from DFT-based calculations.

2.2. Quantum Transport via NN-TP Molecules Embedded in a Si-Based Double-Tunnel Junction. A Si-based double-tunnel junction, which comprises Au/aluminum oxide (Al_2O_3)/NN-TP molecules/silicon dioxide (SiO_2), was prepared on highly doped Si substrates, where NN-TP molecules are used as quantum dots (**Figure 1**). The insulating layers (Al_2O_3 and SiO_2) serve as the tunnel barriers, and the Si substrate serves as the bottom electrode. Our previous studies revealed that the tunneling current reflecting the occupied MOs appears in the negative voltage range for a p-type Si substrate because the holes are transported from the bottom Si substrate to the embedded molecules. However, electron tunneling through unoccupied MOs occurs in the positive voltage range when an n-type Si substrate is employed.⁴⁴ Another important point concerning carrier transport is that the quantum transport via molecules in a double-tunnel junction is given by the effects of discrete MOs and the charging energy of embedded molecules.^{42,49,50} The electro-chemical potential $U(N)$ of a molecule can be described using eq 1:

$$U(N) = \varepsilon_N + \frac{e^2}{C} \left(N - \frac{1}{2} \right), \quad (1)$$

where C , N , and ε_N are the capacitance of the double-tunnel-junction, total number of electrons, and energy level of the N^{th} electron, respectively. The energy required to transport a single electron via the discrete energy levels ($N \rightarrow N+1$) is given by Equation 2:

$$\mu(N) = U(N+1) - U(N) = (\varepsilon_{N+1} - \varepsilon_N) + \frac{e^2}{C}, \quad (2)$$

where $\Delta\varepsilon = \varepsilon_{N+1} - \varepsilon_N$ represents the HOMO–LUMO gap of the molecules. When the effect of the charging energy is dominant, the staircases are observed at regular intervals. However, if resonant tunneling is dominant, the staircases are visible with nonuniform intervals, in line with discrete MOs.

The I – V characteristics of a sample with a p-type Si substrate are illustrated in **Figure 3a**; I – V characteristics were measured for 112 devices. The temperature was fixed at 7 K. **Figure 3b** depicts the corresponding differential conductance (dI/dV) curve obtained for the same sample at 7 K. Clear staircases in the I – V curve and sharp peaks in the dI/dV curve were detected at -0.75 V and -0.94 V as indicated by the green arrows in **Figure 3a** and **3b**. The observation yield for the dI/dV peaks was approximately 18% (20 of 112 devices). Notably, the interval of each dI/dV peak is nonuniform, implying that resonant tunneling through discrete MOs of the NN-TP molecules is more dominant than the SET induced by the charging energy. In contrast, no peaks are observed in the dI/dV curve of the reference sample without NN-TP molecules (Au/ Al_2O_3 / SiO_2 /p-type Si) (**Figure S6**). Accordingly, the dI/dV peak at -0.75 V is assigned to

the HOMO of the NN-TP molecules, whereas the dI/dV peak at -0.94 V is assigned to the HOMO-1 of the NN-TP molecules. Furthermore, an n-type Si substrate was used to investigate electron tunneling through the unoccupied MOs of the NN TP molecules. **Figure 3c** and **3d** depict the $I-V$ and dI/dV characteristics of the sample with the n-type Si substrate. The temperature was 7 K. Clear staircases in the $I-V$ and dI/dV peaks are observed at $+0.84$ and $+1$ V, as indicated by the red arrows in Figure 3c and 3d. The two peaks in the positive voltage range are assigned as the LUMO and LUMO+1 of the NN-TP molecules, respectively. The observation yield in case of these MOs is almost same as that in case of the HOMO and HOMO-1 of the NN-TP molecules (approximately 19%; 21 of 112 devices).

The HOMO and LUMO levels calculated from the statistical dI/dV curves are -5.83 ± 0.04 eV and -4.26 ± 0.04 eV, respectively (**Figure S7a** in the Supporting Information). Accordingly, the HOMO-LUMO gap is estimated to be 1.57 eV. Notably, the experimentally obtained HOMO-LUMO gap is different from the theoretical value (3.25 eV). This discrepancy can be attributed to the use of the freestanding configuration of the NN-TP molecule in the theoretical calculations.

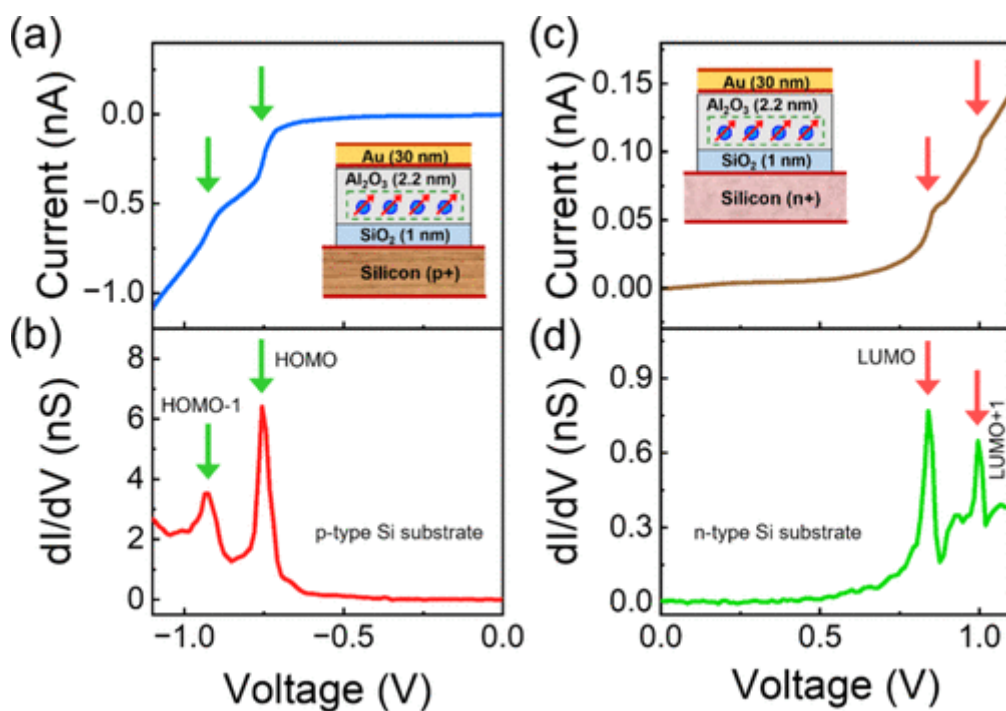


Figure 3. (a) $I-V$ and (b) dI/dV curves of the double-tunnel junction with NN-TP molecules, where the p-type Si substrate was used. (c) $I-V$ and (d) dI/dV curves of the device with the n-type Si substrate. In panels (a-d), the temperature was fixed at 7 K.

An additional staircase and dI/dV peak are visible at -0.34 V in the $I-V$ curves of the

devices with p-type Si substrates, although the yield was as low as 3% (**Figure 4**). Our theoretical calculation of the MOs of NN-TP molecules indicates that the unpaired electronic states (SOMO and SUMO) are located in the HOMO–LUMO gap (**Figure 2b**). In particular, the SOMO is located close to the HOMO. Conversely, the SUMO is located near the LUMO. Hence, the dI/dV peak at -0.34 V is assigned as the SOMO of the NN-TP molecules. Similar carrier transport through a SOMO or SUMO has been observed by STM measurements with open-shell graphene nanoribbons⁵¹ and tetracyano-p-quinodimethane molecules.⁵² In both cases, the dI/dV peak for the SOMO is observed in the negative voltage range, whereas the peak for the SUMO is observed in the positive voltage range.^{51,52} These reports indicate that the dI/dV peak at -0.34 V is caused by the resonant tunneling via the SOMO states of the NN-TP molecules. Accordingly, the SOMO level is estimated to be -5.43 ± 0.02 eV (**Figure S7b**).

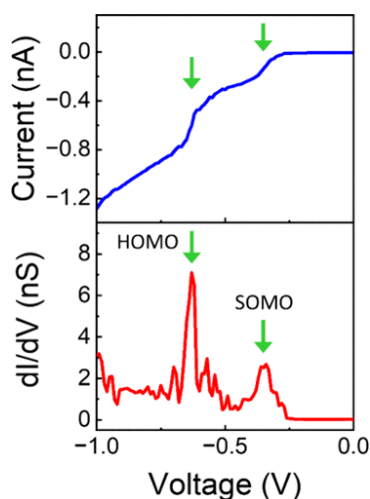


Figure 4. I – V and dI/dV curves of a sample with a p-type Si substrate embedded with NN-TP molecules, where two clear peaks were visible at -0.34 and -0.64 V, respectively. This measurement was performed at 7 K. The dI/dV peak at -0.34 V indicates the resonant tunneling through the SOMO of the NN-TP molecules.

In single molecular junctions and SAM-based junctions, the effect of SOMOs on quantum transport is usually marginal owing to the considerable energy-level broadening of radical molecules. For instance, in $[\text{Ru}2^{\text{H}}]^+$ radical-based SAMs, energy-level broadening occurs owing to strong coupling between the molecules and attached electrodes, resulting in the delocalization of unpaired electrons over the whole molecules.⁵³ However, in our study, a clear dI/dV peak for SOMO was visible, exhibiting that the unpaired electron of the NN-TP molecules is localized in the NN group because the NN-TP molecules are embedded in insulating layers and do not contact the metal electrodes. Furthermore, the observation of the

dI/dV peak for the SOMO is direct evidence that the unpaired electron of the NN-TP molecules remains intact within the Si-based double-tunnel junction. This represents an important advancement in the field of spintronics because spin-polarized MOs (SOMO and SUMO) play a pivotal role in the induction of spin-dependent carrier transport properties.

Next, we examined the device-to-device variation of tunneling characteristics and breakdown voltage to determine device stability. **Figure S9** depicts the device-to-device variations of dI/dV peaks for the MOs of NN-TP. The change in peak positions is considerably small and within ± 0.1 V for all devices. In addition, the breakdown voltage is the maximum applied voltage before device failure.^{54,55} The breakdown voltage of our device is 4.7 V in the positive voltage range (**Figure S10a**) and -5.0 V in the negative voltage range (**Figure S10b**). The large breakdown voltage indicates the stability of our devices within the voltage range of ± 4.0 V.

Studies on single molecular junctions and SAM-based junctions have revealed the difficulty to investigate charge transport through deep MOs such as HOMO-1 and LUMO +1 due to the narrow bias windows,⁵⁶⁻⁵⁸ despite the fact that stronger resonance than frontier MO (HOMO and LUMO) is likely to appear in the deep MOs (HOMO-1 and LUMO+1). Conversely, in our device, the voltage can be applied up to ± 4 V, enabling the observation of resonant tunneling through deeper MOs. In our study, the dI/dV peaks for the deep MOs, including HOMO-1 and LUMO+1, are distinctly observed, providing a clear advantage for using our device. **Figure 5** depicts the carrier transport mechanism through the NN-TP molecules in the Si-based double-tunnel junction. Upon applying negative voltages to the Au electrode, holes are transported from the Si substrate to the occupied MOs (HOMO and HOMO-1) of the NN-TP molecules (**Figure 5a**). Notably, upon applying a small negative voltage to the Au electrode, hole tunneling occurs via the SOMO (**Figure 5b**). Conversely, upon applying positive voltages to the Au electrode, electron tunneling occurs from the Si substrate to the unoccupied MOs (LUMO and LUMO+1) of the NN-TP molecules (**Figure 5c**).

2.3. Temperature Dependence of Quantum Transport via NN-TP Molecules Embedded in a Si-based Double-tunnel Junction. We evaluated the temperature dependence of the $I-V$ and dI/dV curves of the Si-based double-tunnel junction with NN-TP molecules. The examination of the quantum transport in the radical-based molecular junctions is often limited to an extremely low temperature of <15 K because the molecular junctions formed by the break junction and STM techniques are unstable.^{22-24,38,59,60} **Figure 6a** and **6b** depict the temperature

dependence of the I – V and dI/dV curves for the sample with the p-type Si substrate. The staircases in the I – V curve and the dI/dV peaks observed at 7 K are visible up to 100 K – a higher temperature than previously reported.^{22,23,59}

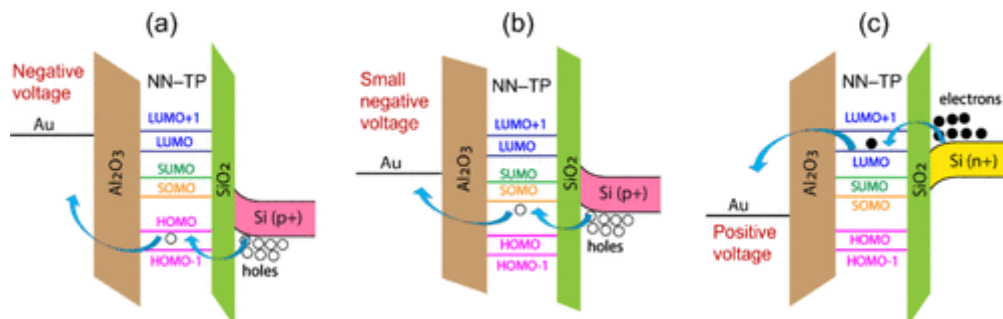


Figure 5. Carrier transport mechanism through (a) fully occupied (HOMO), (b) SOMO, and (c) fully unoccupied (LUMO) MOs in the Si-based double-tunnel junction with NN-TP molecules.

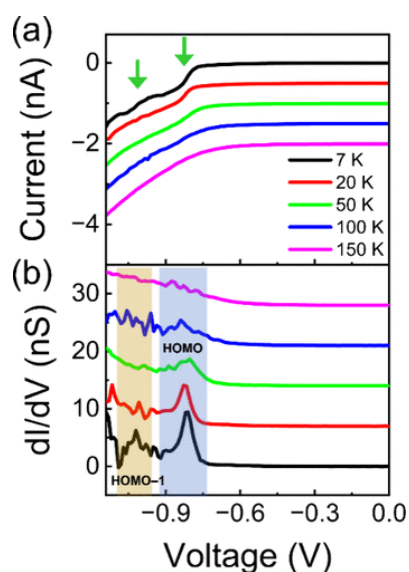


Figure 6. Temperature dependence of (a) I – V and (b) dI/dV curves in the sample with NN-TP molecules, wherein the p-type Si substrate was used. The temperature varied from 7 to 150 K. Notably, the I – V and dI/dV curves have been vertically shifted for better visibility.

Furthermore, the estimated activation energy of the tunneling current is below 1 mV at < 50 K (**Figure S11** in the Supporting Information), although the energy increases to 3–5 mV at > 50 K. These results show that the transport mechanism is dominated by resonant tunneling below 50 K.^{61–65}

However, broadening of the staircases in the I – V curve and the dI/dV peaks occurs with

increasing temperature. Peak broadening in the dI/dV curve occurs owing to the thermal broadening of the Fermi edge. Another possible reason is the thermal vibration of the embedded molecules. In both cases, peak broadening is in the order of $k_B T$ (k_B is the Boltzmann constant). However, for our sample, the full width at half maximum (FWHM) of the dI/dV peak for the HOMO (**Figure S12**) indicates peak broadening larger than the order of $k_B T$. The FWHM of the dI/dV peak for the HOMO increases from 54 mV at 7 K to 117 mV at 100 K. Thus, other factors also affect peak broadening. Speculatively, broadening of the dI/dV peaks results from the interaction between the molecular orbital and insulating layer.⁶⁶

3. CONCLUSIONS

We demonstrated resonant tunneling through purely organic radical molecules (NN-TP), where the molecules were employed as quantum dots in an MOS structure. The clear staircases in the $I-V$ curves and prominent peaks in the dI/dV curves are ascribed to multilevel resonant tunneling through discrete MOs of the NN-TP molecules at 7 K. Quantum transport was observed even at 100 K. Furthermore, we successfully observed resonant tunneling through the SOMO. This phenomenon demonstrates the survival of the unpaired electrons in the NN-TP molecules within the solid-state device. Our findings provide a foundation for further investigations into spin transport through organic radicals in Si-based double-tunnel junctions. This could ultimately lead to the development of CMOS-compatible molecular spintronic devices.

4. MATERIALS AND METHODS

4.1. Synthesis of NN-TP Molecules. The synthesis of NN-TP molecules is depicted in the Supporting Information (Section 1).

4.2. Device Fabrication. A Si-based double-tunnel junction was prepared on highly doped Si (100) substrates, where isolated NN-TP molecules were sandwiched between the ultrathin SiO_2 and Al_2O_3 insulating layers. First, a highly doped Si substrate was cleaned in acetone and isopropanol through ultrasonication for 5 min and rinsed with ultrapure water. Subsequently, the substrate was ultraviolet ozone treated. The cleaned substrate was then immersed in dilute hydrofluoric acid for hydrogen termination, rinsed with deionized water, and dried using N_2 flow. A SiO_2 layer was then formed as the first tunnel layer via thermal annealing at 500 °C. Subsequently, the SiO_2/Si substrate was placed in a high-vacuum molecule deposition chamber. The NN-TP molecules were thermally evaporated on the SiO_2 surface under 1×10^{-6} Pa. The

deposition rate and time were 0.45 Å/ min and 1.5 min, respectively. The number density of the molecules was estimated to be in the order of $10^{12} - 10^{13} \text{ cm}^{-2}$ based on our previous study.⁴² The sample was transferred into an atomic layer deposition chamber without breaking the high vacuum condition. Subsequently, a 2.2 nm-thick Al₂O₃ film was formed on the NN-TP molecules. The Al₂O₃ film not only served as the second tunnel layer but also protected the molecules from exposure to the ambient environment. Finally, the top circular electrodes (gold) with a diameter of 500 µm were deposited through a metal shadow mask using a thermal deposition system.

4.3. Electrical Measurements. *I*–*V* measurements were performed using a semiconductor parameter analyzer (Keysight Technology, B2912B) in a low-temperature probe system (Nagase Techno-Engineering Co. Ltd.). The voltages were applied to the top gold electrode while the bottom Si substrate was grounded. The temperature varied between 5 and 300 K.

■ ASSOCIATED CONTENT

Supporting Information

The Supporting Information is available free of charge at <https://pubs.acs.org/doi/10.1021/acsami.5c00839>.

Synthesis and characterization of NN-TP molecules, molecular orbital calculations of the reference molecule without the radical part, molecular orbital calculation of NN-TP molecules, *I*–*V* characteristics of the reference device without NN-TP molecules, statistical distribution of *dI/dV* peak positions associated with the HOMO, LUMO, and SOMO, optimization of film thickness of Al₂O₃ layer, device-to-device variation of tunneling characteristics, evaluation of breakdown voltage, activation energy of tunneling current, and variation in FWHM of HOMO peak with temperature (PDF).

■ AUTHOR INFORMATION

Corresponding Authors

Thomas Huhn – Department of Chemistry, University of Konstanz, Konstanz 78457, Germany; orcid.org/0000 0001-6292-4215; Email: thomas.huhn@uni-konstanz.de

Ryoma Hayakawa – Quantum Device Engineering Group, Research Center for Materials Nanoarchitectonics (MANA), National Institute for Materials Science (NIMS), Tsukuba, Ibaraki 305-0044, Japan; orcid.org/0000-0002-1442 8230; Email: HAYAKAWA.Ryoma@nims.go.jp

Authors

Jayanta Bera – Quantum Device Engineering Group, Research Center for Materials Nanoarchitectonics (MANA), National Institute for Materials Science (NIMS), Tsukuba, Ibaraki 305-0044, Japan

Mikhail Kabdulov – Department of Chemistry, University of Konstanz, Konstanz 78457, Germany

Yutaka Wakayama – Quantum Device Engineering Group, Research Center for Materials Nanoarchitectonics (MANA), National Institute for Materials Science (NIMS), Tsukuba, Ibaraki 305-0044, Japan; orcid.org/0000-0002-0801-8884

Complete contact information is available at: <https://pubs.acs.org/10.1021/acsami.5c00839>

Author Contributions

The manuscript was written through the contributions of all authors. All authors have given approval to the final version of the manuscript.

Notes

The authors declare no competing financial interest.

■ ACKNOWLEDGMENTS

This research was supported by the World Premier International Center (WPI) for Materials Nanoarchitectonics (MANA) of the National Institute for Materials Science (NIMS), JSPS KAKENHI grant numbers 23K22802 and 24KF0270, and Advanced Research Infrastructure for Materials and Nanotechnology in Japan (ARIM) of the Ministry of Education, Culture, Sports, Science and Technology (MEXT), grant number JPMXP1223NM5170.

■ REFERENCES

- (1) Gao, S.; Yi, X.; Shang, J.; Liu, G.; Li, R.-W. Organic and Hybrid Resistive Switching Materials and Devices. *Chem. Soc. Rev.* 2019, 48 (6), 1531–1565.
- (2) Lv, Z.; Wang, Y.; Chen, J.; Wang, J.; Zhou, Y.; Han, S.-T. Semiconductor Quantum Dots for Memories and Neuromorphic Computing Systems. *Chem. Rev.* 2020, 120 (9), 3941–4006.
- (3) Cho, B.; Song, S.; Ji, Y.; Kim, T.-W.; Lee, T. Organic Resistive Memory Devices:

Performance Enhancement, Integration, and Advanced Architectures. *Adv. Funct. Mater.* 2011, 21 (15), 2806–2829.

(4) Ielmini, D.; Wong, H.-S. P. In-Memory Computing with Resistive Switching Devices. *Nat. Electron* 2018, 1 (6), 333–343.

(5) Chen, Z.; Grace, I. M.; Woltering, S. L.; Chen, L.; Gee, A.; Baugh, J.; Briggs, G. A. D.; Bogani, L.; Mol, J. A.; Lambert, C. J.; Anderson, H. L.; Thomas, J. O. Quantum Interference Enhances the Performance of Single-Molecule Transistors. *Nat. Nanotechnol.* 2024, 19 (7), 986–992.

(6) Capozzi, B.; Xia, J.; Adak, O.; Dell, E. J.; Liu, Z.-F.; Taylor, J. C.; Neaton, J. B.; Campos, L. M.; Venkataraman, L. Single-Molecule Diodes with High Rectification Ratios through Environmental Control. *Nat. Nanotechnol.* 2015, 10 (6), 522–527.

(7) Lörtscher, E.; Gotsmann, B.; Lee, Y.; Yu, L.; Rettner, C.; Riel, H. Transport Properties of a Single-Molecule Diode. *ACS Nano* 2012, 6 (6), 4931–4939.

(8) Batra, A.; Darancet, P.; Chen, Q.; Meisner, J. S.; Widawsky, J. R.; Neaton, J. B.; Nuckolls, C.; Venkataraman, L. Tuning Rectification in Single-Molecular Diodes. *Nano Lett.* 2013, 13 (12), 6233–6237.

(9) Brooke, R. J.; Jin, C.; Szumski, D. S.; Nichols, R. J.; Mao, B.-W.; Thygesen, K. S.; Schwarzacher, W. Single-Molecule Electrochemical Transistor Utilizing a Nickel-Pyridyl Spinterface. *Nano Lett.* 2015, 15 (1), 275–280.

(10) Perrin, M. L.; Burzurí, E.; van der Zant, H. S. J. Single-Molecule Transistors. *Chem. Soc. Rev.* 2015, 44 (4), 902–919.

(11) Martínez-Blanco, J.; Nacci, C.; Erwin, S. C.; Kanisawa, K.; Locane, E.; Thomas, M.; von Oppen, F.; Brouwer, P. W.; Fölsch, S. Gating a Single-Molecule Transistor with Individual Atoms. *Nat. Phys.* 2015, 11 (8), 640–644.

(12) Ho Choi, S.; Kim, B.; Frisbie, C. D. Electrical Resistance of Long Conjugated Molecular Wires. *Science* 2008, 320 (5882), 1482–1486.

(13) Choi, B.-Y.; Kahng, S.-J.; Kim, S.; Kim, H.; Kim, H. W.; Song, Y. J.; Ihm, J.; Kuk, Y. Conformational Molecular Switch of the Azobenzene Molecule: A Scanning Tunneling Microscopy Study. *Phys. Rev. Lett.* 2006, 96 (15), No. 156106.

(14) Quek, S. Y.; Kamenetska, M.; Steigerwald, M. L.; Choi, H. J.; Louie, S. G.; Hybertsen, M. S.; Neaton, J. B.; Venkataraman, L. Mechanically Controlled Binary Conductance Switching of a Single Molecule Junction. *Nat. Nanotechnol.* 2009, 4 (4), 230–234.

(15) Sanvito, S. Spintronics Goes Plastic. *Nat. Mater.* 2007, 6 (11), 803–804.

- (16) Pramanik, S.; Stefanita, C.-G.; Patibandla, S.; Bandyopadhyay, S.; Garre, K.; Harth, N.; Cahay, M. Observation of Extremely Long Spin Relaxation Times in an Organic Nanowire Spin Valve. *Nat. Nanotechnol.* 2007, 2 (4), 216–219.
- (17) Rugg, B. K.; Krzyaniak, M. D.; Phelan, B. T.; Ratner, M. A.; Young, R. M.; Wasielewski, M. R. Photodriven Quantum Teleportation of an Electron Spin State in a Covalent Donor–Acceptor–Radical System. *Nat. Chem.* 2019, 11 (11), 981–986.
- (18) Nelson, J. N.; Krzyaniak, M. D.; Horwitz, N. E.; Rugg, B. K.; Phelan, B. T.; Wasielewski, M. R. Zero Quantum Coherence in a Series of Covalent Spin-Correlated Radical Pairs. *J. Phys. Chem. A* 2017, 121 (11), 2241–2252.
- (19) Miura, T.; Wasielewski, M. R. Manipulating Photogenerated Radical Ion Pair Lifetimes in Wirelike Molecules Using Microwave Pulses: Molecular Spintronic Gates. *J. Am. Chem. Soc.* 2011, 133 (9), 2844–2847.
- (20) Tesi, L.; Stemmler, F.; Winkler, M.; Liu, S. S. Y.; Das, S.; Sun, X.; Zharnikov, M.; Ludwigs, S.; van Slageren, J. Modular Approach to Creating Functionalized Surface Arrays of Molecular Qubits. *Adv. Mater.* 2023, 35 (10), No. 2208998.
- (21) Li, L.; Prindle, C. R.; Shi, W.; Nuckolls, C.; Venkataraman, L. Radical Single-Molecule Junctions. *J. Am. Chem. Soc.* 2023, 145 (33), 18182–18204.
- (22) Frisenda, R.; Gaudenzi, R.; Franco, C.; Mas-Torrent, M.; Rovira, C.; Veciana, J.; Alcon, I.; Bromley, S. T.; Burzuri, E.; van der Zant, H. S. J. Kondo Effect in a Neutral and Stable All Organic Radical Single Molecule Break Junction. *Nano Lett.* 2015, 15 (5), 3109–3114.
- (23) Mitra, G.; Low, J. Z.; Wei, S.; Francisco, K. R.; Deffner, M.; Herrmann, C.; Campos, L. M.; Scheer, E. Interplay between Magnetoresistance and Kondo Resonance in Radical Single-Molecule Junctions. *Nano Lett.* 2022, 22 (14), 5773–5779.
- (24) Hayakawa, R.; Karimi, M. A.; Wolf, J.; Huhn, T.; Zöllner, M. S.; Herrmann, C.; Scheer, E. Large Magnetoresistance in Single-Radical Molecular Junctions. *Nano Lett.* 2016, 16 (8), 4960–4967.
- (25) Xu, B.; Tao, N. J. Measurement of Single-Molecule Resistance by Repeated Formation of Molecular Junctions. *Science* 2003, 301 (5637), 1221–1223.
- (26) Dief, E. M.; Low, P. J.; Díez-Pérez, I.; Darwish, N. Advances in Single-Molecule Junctions as Tools for Chemical and Biochemical Analysis. *Nat. Chem.* 2023, 15 (5), 600–614.
- (27) Liu, Z.; Ding, S.-Y.; Chen, Z.-B.; Wang, X.; Tian, J.-H.; Anema, J. R.; Zhou, X.-S.; Wu, D.-Y.; Mao, B.-W.; Xu, X.; Ren, B.; Tian, Z.-Q. Revealing the Molecular Structure of Single-

Molecule Junctions in Different Conductance States by Fishing-Mode Tip-Enhanced Raman Spectroscopy. *Nat. Commun.* 2011, 2 (1), 305.

(28) Warner, B.; El Hallak, F.; Prüser, H.; Sharp, J.; Persson, M.; Fisher, A. J.; Hirjibehedin, C. F. Tunable Magnetoresistance in an Asymmetrically Coupled Single-Molecule Junction. *Nat. Nanotechnol.* 2015, 10 (3), 259–263.

(29) Yang, K.; Chen, H.; Pope, T.; Hu, Y.; Liu, L.; Wang, D.; Tao, L.; Xiao, W.; Fei, X.; Zhang, Y.-Y.; Luo, H.-G.; Du, S.; Xiang, T.; Hofer, W. A.; Gao, H.-J. Tunable Giant Magnetoresistance in a Single-Molecule Junction. *Nat. Commun.* 2019, 10 (1), 3599.

(30) Willke, P.; Bilgeri, T.; Zhang, X.; Wang, Y.; Wolf, C.; Aubin, H.; Heinrich, A.; Choi, T. Coherent Spin Control of Single Molecules on a Surface. *ACS Nano* 2021, 15 (11), 17959–17965.

(31) Xiang, D.; Jeong, H.; Lee, T.; Mayer, D. Mechanically Controllable Break Junctions for Molecular Electronics. *Adv. Mater.* 2013, 25 (35), 4845–4867.

(32) Parks, J. J.; Champagne, A. R.; Hutchison, G. R.; Flores-Torres, S.; Abruña, H. D.; Ralph, D. C. Tuning the Kondo Effect with a Mechanically Controllable Break Junction. *Phys. Rev. Lett.* 2007, 99 (2), No. 026601.

(33) Bruot, C.; Hihath, J.; Tao, N. Mechanically Controlled Molecular Orbital Alignment in Single Molecule Junctions. *Nat. Nanotechnol.* 2012, 7 (1), 35–40.

(34) Gehring, P.; Thijssen, J. M.; van der Zant, H. S. J. Single Molecule Quantum-Transport Phenomena in Break Junctions. *Nat. Rev. Phys.* 2019, 1 (6), 381–396.

(35) Aradhya, S. V.; Frei, M.; Halbritter, A.; Venkataraman, L. Correlating Structure, Conductance, and Mechanics of Silver Atomic Scale Contacts. *ACS Nano* 2013, 7 (4), 3706–3712.

(36) Reed, M. A.; Zhou, C.; Muller, C. J.; Burgin, T. P.; Tour, J. M. Conductance of a Molecular Junction. *Science* 1997, 278 (5336), 252–254.

(37) Naghibi, S.; Sangtarash, S.; Kumar, V. J.; Wu, J.-Z.; Judd, M. M.; Qiao, X.; Gorenskaia, E.; Higgins, S. J.; Cox, N.; Nichols, R. J.; Sadeghi, H.; Low, P. J.; Vezzoli, A. Redox-Addressable Single Molecule Junctions Incorporating a Persistent Organic Radical. *Angew. Chem., Int. Ed.* 2022, 61 (23), No. e202116985.

(38) Baum, T. Y.; Fernández, S.; Peña, D.; van der Zant, H. S. J. Magnetic Fingerprints in an All-Organic Radical Molecular Break Junction. *Nano Lett.* 2022, 22 (20), 8086–8092.

(39) Song, H.; Kim, Y.; Jang, Y. H.; Jeong, H.; Reed, M. A.; Lee, T. Observation of Molecular Orbital Gating. *Nature* 2009, 462 (7276), 1039–1043.

- (40) Yasutake, Y.; Shi, Z.; Okazaki, T.; Shinohara, H.; Majima, Y. Single Molecular Orientation Switching of an Endohedral Metal Iofullerene. *Nano Lett.* 2005, 5 (6), 1057–1060.
- (41) Nakaya, M.; Tsukamoto, S.; Kuwahara, Y.; Aono, M.; Nakayama, T. Molecular Scale Control of Unbound and Bound C 60 for Topochemical Ultradense Data Storage in an Ultrathin C Adv. Mater. 2010, 22 (14), 1622–1625. 60 Film.
- (42) Hayakawa, R.; Hiroshiba, N.; Chikyow, T.; Wakayama, Y. Single-Electron Tunneling through Molecular Quantum Dots in a Metal-Insulator-Semiconductor Structure. *Adv. Funct. Mater.* 2011, 21 (15), 2933–2937.
- (43) Hayakawa, R.; Higashiguchi, K.; Matsuda, K.; Chikyow, T.; Wakayama, Y. Photoisomerization-Induced Manipulation of Single Electron Tunneling for Novel Si-Based Optical Memory. *ACS Appl. Mater. Interfaces* 2013, 5 (21), 11371–11376.
- (44) Hayakawa, R.; Chikyow, T.; Wakayama, Y. Vertical Resonant Tunneling Transistors with Molecular Quantum Dots for Large-Scale Integration. *Nanoscale* 2017, 9 (31), 11297–11302.
- (45) Kohn, W.; Sham, L. J. Self-Consistent Equations Including Exchange and Correlation Effects. *Phys. Rev.* 1965, 140 (4A), A1133–A1138.
- (46) Perdew, J. P.; Burke, K.; Ernzerhof, M. Generalized Gradient Approximation Made Simple. *Phys. Rev. Lett.* 1996, 77 (18), 3865–3868.
- (47) Neese, F.; Wennmohs, F.; Becker, U.; Riplinger, C. The ORCA Quantum Chemistry Program Package. *J. Chem. Phys.* 2020, 152 (22), No. 224108.
- (48) Grimme, S.; Antony, J.; Ehrlich, S.; Krieg, H. A Consistent and Accurate Ab Initio Parametrization of Density Functional Dispersion Correction (DFT-D) for the 94 Elements H-Pu. *J. Chem. Phys.* 2010, 132 (15), No. 154104.
- (49) Porath, D.; Millo, O. Single Electron Tunneling and Level Spectroscopy of Isolated C 60 2241–2244. *Molecules. J. Appl. Phys.* 1997, 81 (5),
- (50) Beenakker, C. W. J.; Van Houten, H.; Staring, A. A. M. Influence of Coulomb Repulsion on the Aharonov-Bohm Effect in a Quantum Dot. *Phys. Rev. B* 1991, 44 (4), 1657–1662.
- (51) Wang, T.; Sanz, S.; Castro-Esteban, J.; Lawrence, J.; Berdonces Layunta, A.; Mohammed, M. S. G.; Vilas-Varela, M.; Corso, M.; Peña, D.; Frederiksen, T.; de Oteyza, D. G. Magnetic Interactions Between Radical Pairs in Chiral Graphene Nanoribbons. *Nano Lett.* 2022, 22 (1), 164–171.
- (52) Garnica, M.; Stradi, D.; Barja, S.; Calleja, F.; Díaz, C.; Alcamí, M.; Martín, N.; Vázquez de Parga, A. L.; Martín, F.; Miranda, R. Long-Range Magnetic Order in a Purely Organic 2D

Layer Adsorbed on Epitaxial Graphene. *Nat. Phys.* 2013, 9 (6), 368–374.

(53) Park, S.; Jang, J.; Tanaka, Y.; Yoon, H. J. High Seebeck Coefficient Achieved by Multinuclear Organometallic Molecular Junctions. *Nano Lett.* 2022, 22 (23), 9693–9699.

(54) Kong, G. D.; Song, H.; Yoon, S.; Kang, H.; Chang, R.; Yoon, H. J. Interstitially Mixed Self-Assembled Monolayers Enhance Electrical Stability of Molecular Junctions. *Nano Lett.* 2021, 21 (7), 3162–3169.

(55) Yuan, L.; Jiang, L.; Nijhuis, C. A. The Drive Force of Electrical Breakdown of Large-Area Molecular Tunnel Junctions. *Adv. Funct. Mater.* 2018, 28 (28), No. 1801710.

(56) Jang, J.; Kong, G. D.; Yoon, H. J. Electrically Stable Self Assembled Monolayers Achieved through Repeated Surface Exchange of Molecules. *Acc. Mater. Res.* 2024, 5 (10), 1251–1262.

(57) Kong, G. D.; Jang, J.; Choi, S.; Lim, G.; Kim, I. S.; Ohto, T.; Maeda, S.; Tada, H.; Yoon, H. J. Dynamic Variation of Rectification Observed in Supramolecular Mixed Mercaptoalkanoic Acid. *Small* 2024, 20 (5), No. 2305997.

(58) Kong, G. D.; Byeon, S. E.; Jang, J.; Kim, J. W.; Yoon, H. J. Electronic Mechanism of In Situ Inversion of Rectification Polarity in Supramolecular Engineered Monolayer. *J. Am. Chem. Soc.* 2022, 144 (18), 7966–7971.

(59) Bejarano, F.; Olavarria-Contreras, I. J.; Droghetti, A.; Rungger, I.; Rudnev, A.; Gutiérrez, D.; Mas-Torrent, M.; Veciana, J.; van der Zant, H. S. J.; Rovira, C.; Burzurí, E.; Crivillers, N. Robust Organic Radical Molecular Junctions Using Acetylene Terminated Groups for C–Au Bond Formation. *J. Am. Chem. Soc.* 2018, 140 (5), 1691–1696.

(60) Patera, L. L.; Sokolov, S.; Low, J. Z.; Campos, L. M.; Venkataraman, L.; Repp, J. Resolving the Unpaired-Electron Orbital Distribution in a Stable Organic Radical by Kondo Resonance Mapping. *Angew. Chem., Int. Ed.* 2019, 58 (32), 11063–11067.

(61) Jang, J.; Yoon, H. J. Long-Range Charge Transport in Molecular Wires. *J. Am. Chem. Soc.* 2024, 146 (47), 32206–32221.

(62) Jang, J.; Jo, J. W.; Ohto, T.; Yoon, H. J. Seebeck Effect in Molecular Wires Facilitating Long-Range Transport. *J. Am. Chem. Soc.* 2024, 146 (7), 4922–4929.

(63) Lee, H. J.; Cho, S. J.; Kang, H.; He, X.; Yoon, H. J. Achieving Ultralow, Zero, and Inverted Tunneling Attenuation Coefficients in Molecular Wires with Extended Conjugation. *Small* 2021, 17 (12), No. 2005711.

(64) Ouyang, C.; Hashimoto, K.; Tsuji, H.; Nakamura, E.; Majima, Y. Coherent Resonant Electron Tunneling at 9 and 300 K through a 4.5 nm Long, Rigid, Planar Organic Molecular

Wire. ACS Omega 2018, 3 (5), 5125–5130.

(65) Kuang, G.; Chen, S.-Z.; Wang, W.; Lin, T.; Chen, K.; Shang, X.; Liu, P. N.; Lin, N. Resonant Charge Transport in Conjugated Molecular Wires beyond 10 Nm Range. J. Am. Chem. Soc. 2016, 138 (35), 11140–11143.

(66) Basu, T. S.; Wakayama, Y.; Hayakawa, R. Theoretical Insight into Quantum Transport Via Molecular Dots in a Vertical Tunnel Transistor. ACS Appl. Electron. Mater. 2021, 3 (2), 973–978.